

Low-Noise Active-RC Low-, High- and Band-Pass Allpole Filters using Impedance Tapering

Dražen Jurišić and George S. Moschytz, *Fellow, IEEE*

Abstract—It is shown that low-sensitivity active resistance-capacitance (RC) filters are also low in output thermal noise. The design procedure of second- and third-order low-sensitivity allpole filters, using impedance tapering, has already been published. The component values selected for impedance tapering account for the considerable decrease in output thermal noise. The method of Zurada and Bialko was used to determine output noise spectral density and total rms output noise of filters. Passive elements and operational amplifier are represented by substitute noise models. The noise contribution of each device to the output node is calculated using noise transfer functions. The noise analysis was performed on the second-order (class 4) Sallen and Key low-pass, high-pass and band-pass filter sections using MATLAB. The extension to third- and higher-order filters follows the same principles. It was found that the filters with minimum noise coincide with the filters with minimum sensitivity to component tolerances.

Index Terms— Allpole filters, impedance tapering, low-noise active filters, low-sensitivity active filters.

I. INTRODUCTION

The quality of low signal-level and low-power signal processing, depends, among other factors, on the noise level produced in the circuits. In filter circuits it is especially important to have the noise level as low as possible.

In this paper we demonstrate that allpole active-RC filters of second-order that are designed for minimum sensitivity to component tolerances are also superior in terms of low output thermal noise, when compared with standard designs. Low-pass, high-pass and band-pass filters are considered. The extension of lowering noise as well as lowering sensitivity by impedance tapering, to third- and higher-order filters follows the same principles as those presented here. The improvement is considerable and comes free of charge, in that it requires simply the same selection of appropriate component values, based on “impedance tapering”, as was described in [5] and [6].

Noise effects are calculated using the transfer function with respect to each noise source as shown in [1] and [2]. As a dynamic range (D_R) measure the ratio of maximum

undistorted voltage level and the RMS noise within a specified frequency range is used [4].

II. LOW-SENSITIVITY ALLPOLE FILTERS USING IMPEDANCE TAPERING

A procedure for the design of low-pass allpole filters with low sensitivity to component tolerances is presented in [5], and for band-pass and high-pass filters in [6]. The presented filter circuits are of low-power because they use only one operational amplifier per circuit.

It is shown that by the use of impedance tapering, in which L-sections of the RC ladder are successively scaled upwards, the sensitivity of the filter characteristics to component tolerances can be significantly decreased. *The design procedure adds nothing to the cost of conventional circuits*; component count and topology remain unchanged, whereas the component values selected for impedance tapering account for a considerable decrease in component tolerance sensitivity. In [5] and [6], a Monte Carlo analysis with PSPICE was performed to examine the sensitivity of the filter’s transfer function on RC component tolerances. In all cases, it is shown that RC tapering reduces the sensitivity of the filter transfer function to RC component tolerances.

III. NOISE AND DYNAMIC RANGE

Active-RC filters consist of resistors, capacitors and operational amplifiers. Thermal noise in resistors is caused by random motion of free charges and is also called Johnson’s noise. Noise in real capacitors is also of thermal origin. It is produced within the resistive non-ideal part of a capacitor, and can be neglected. Because thermal noise is stochastic in nature, we describe its influence by the mean-square noise voltage within a frequency band Δf as follows:

$$\overline{v_n^2} = 4kTR\Delta f, \quad (3.1)$$

or by the mean-square noise current:

$$\overline{i_n^2} = 4kT \frac{1}{R} \Delta f, \quad (3.2)$$

where $k=1.38 \cdot 10^{-23}$ J/K is Boltzman’s constant. Note that thermal noise is proportional to the absolute temperature T .

Let us now define measures by which we can examine the noise performance of the filters under consideration. The most important is the MS noise voltage within a specified frequency range $\Delta\omega=\omega_2-\omega_1$, defined as:

Dražen Jurišić is with the Faculty of Electrical Engineering and Computing, Hr-10000 Zagreb, Croatia.

G.S.Moschytz is with the Swiss Federal Institute of technology, CH-8092, Zurich, Switzerland.

$$(E_n^2)_{ef} = \int_{\omega_1}^{\omega_2} V_n^2(\omega) d\omega, \quad (3.3)$$

where the square of the noise spectral density, derived from all the noise sources and their corresponding transfer functions as given in Table I, is given by:

$$V_n^2(\omega) = \sum_{k=1}^m |T_{i,k}(j\omega)|^2 (i_n)_k^2 + \sum_{l=1}^n |T_{v,l}(j\omega)|^2 (v_n)_l^2 \quad (3.4)$$

where $T_{i,k}(j\omega)$ is a transfer impedance, i.e. the ratio of the output voltage and input current of the k -th current noise source $(i_n)_k$, and $T_{v,l}(j\omega)$ is a voltage transfer function, i.e. ratio of output voltage and input voltage of l -th current voltage source $(v_n)_l$.

For the purpose of noise analysis, appropriate noise models for resistors and operational amplifiers (OAs) must be used. Resistors are represented by the well-known Nyquist current noise model shown in Fig. 1 a) consisting of a noiseless resistor and a noise source whose value is given by eq. (3.2). Noise in operational amplifiers is caused by the built-in semiconductors and resistors. The operational amplifier is represented by the model shown in Fig. 1 b), i.e. a noiseless OA combined with voltage and current noise sources. For the TL081/TI (Texas instruments) operational amplifier approximate values: $E_n = 17 \text{ nV}/\sqrt{\text{Hz}}$ and $I_n = 0.01 \text{ pA}/\sqrt{\text{Hz}}$. These values have been used in the noise analysis presented.

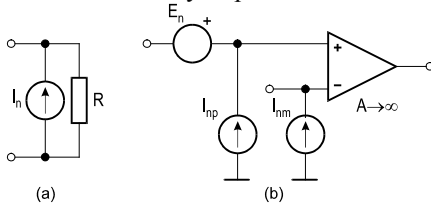


Fig. 1. Substitute Noise Models for: a) Resistor, b) Operational Amplifier (OA).

The impact of noise on the dynamic range of the filter can be given by the measure D_R which is defined as follows:

$$D_R = 20 \log \frac{((V_{OUT})_{ef})_{\max}}{(E_n)_{ef}} \quad [\text{dB}] \quad (3.5)$$

where the numerator represents the maximum undistorted RMS output voltage and the denominator is the RMS noise voltage within a specified frequency range as defined in eq. (3.3).

The RMS noise voltage $(E_n)_{ef}$ was calculated over the frequency range 1kHz–1MHz for all second-order low-pass filter examples. Using the numerical programming tool MATLAB mathematical calculations of the output noise were performed, using the noise transfer functions and simple operations of addition, multiplication, etc. An ideal operational amplifier was replaced by a simple positive voltage gain β , combined with voltage and current noise sources as in Fig. 1.b.

At this point it is very important to stress, that formal proof of the low-noise is the consequence of low-sensitivity.

This goes beyond the scope of this paper and will be researched in future work.

For the D_R calculation an upper and lower limit of the output signal must be known. The upper limit is determined by the slew rate and the corresponding THD for each filter. For the SABB sections this limit depends on the voltage supplied and the OA used [3]. For our examples we used $((V_{OUT})_{ef})_{\max} = 5/\sqrt{2} \text{ V}$.

A. Second-order Low-Pass Filters

Consider the second-order low-pass filter shown in Fig. 2. The voltage gain β is obtained with an ideal non-inverting OA. These circuits are known as class 4 [9] or Sallen & Key [8].

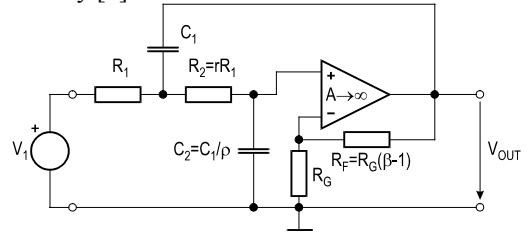


Fig. 2. Second-order Low-pass Filter.

The voltage transfer function $T(s)$ of this section is given in the first line (V_1) in Table I

$$T(s) = \frac{V_{OUT}}{V_1} = \frac{N(s)}{D(s)} = \frac{\beta a_0}{s^2 + a_1 s + a_0}, \quad (3.6)$$

where $D(s)$ is the denominator and is given in the last line of Table I. Note that the gain β is given by:

$$\beta = 1 + \frac{R_F}{R_G}. \quad (3.7)$$

Using the substitute noise models for the resistors and OA, we obtain the configuration shown in Fig. 3. The transfer functions of every noise source to the output voltage is:

$$T_x(s) = \frac{V_{OUT}}{N_x}. \quad (3.8)$$

The noise transfer functions $T_x(s)$ are listed in Table I, where N_x is either the voltage or current noise source of the element denoted by x . The transfer functions were calculated with the help of the symbolic calculation tool MATHEMATICA.

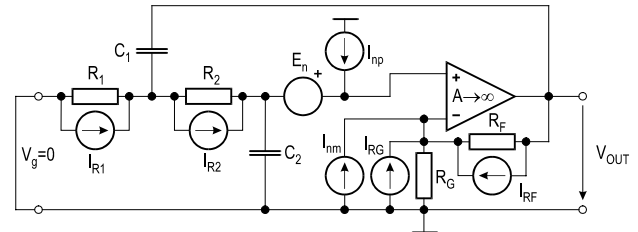


Fig. 3. Noise Sources for Second-order Low-pass Filter.

Example: Consider the following practical example. Suppose that

$$\omega_p = \omega_0 = 2\pi \cdot 86 \text{ kHz}; \quad q_p = 5; \quad C = 500 \text{ pF}. \quad (3.9)$$

In designing filters, various ways of impedance tapering have been applied and the resulting component values are presented in Table II. These are the same examples as in [5]. Monte Carlo runs with 5% Gauss-distribution, zero-mean resistors and capacitors were carried out.

TABLE I
NOISE SOURCE TRANSFER FUNCTIONS FOR SECOND-ORDER LOW-PASS FILTER

N_x	$T_x(s)$
V_1	$\frac{1}{R_1 R_2 C_1 C_2} \left(1 + \frac{R_F}{R_G} \right) / D(s)$
I_{R1}	$\frac{1}{R_2 C_1 C_2} \left(1 + \frac{R_F}{R_G} \right) / D(s)$
I_{R2}	$\left(1 + \frac{R_F}{R_G} \right) \left[\frac{1}{C_2} s + \frac{1}{R_1 C_1 C_2} \right] / D(s)$
I_p	$\left(1 + \frac{R_F}{R_G} \right) \left[\frac{1}{C_2} s + \frac{1}{R_1 C_1 C_2} + \frac{1}{R_2 C_1 C_2} \right] / D(s)$
I_M I_{RG} I_{RF}	$-R_F \left[s^2 + \left(\frac{1}{R_1 C_1} + \frac{1}{R_2 C_1} + \frac{1}{R_2 C_2} \right) s + \frac{1}{R_1 R_2 C_1 C_2} \right] / D(s)$
E	$\left(1 + \frac{R_F}{R_G} \right) \left[s^2 + \left(\frac{1}{R_1 C_1} + \frac{1}{R_2 C_1} + \frac{1}{R_2 C_2} \right) s + \frac{1}{R_1 R_2 C_1 C_2} \right] / D(s)$
	$D(s) = s^2 + \left(\frac{1}{R_1 C_1} + \frac{1}{R_2 C_1} - \frac{R_F}{R_2 C_2 R_G} \right) s + \frac{1}{R_1 R_2 C_1 C_2}$

Using impedance tapering instead of a standard circuit design procedure, the sensitivity of the filter characteristics to component tolerances is significantly decreased. This can be seen in Table III in which the filter's magnitude mean value $\bar{\alpha}(\omega_p)$ and magnitude standard deviation $\sigma_{\alpha}(\omega_p)$ is given. With the noise voltage spectral density calculation using eq. (3.4) and the corresponding dynamic range calculation defined by eqs. (3.3) and (3.5), we obtain the dynamic range for these filters as also presented in Table III.

TABLE II
COMPONENT VALUES OF SECOND-ORDER LOW-PASS FILTERS (RESISTORS IN [kΩ], CAPACITORS IN [pF])

Nr.	Filter	R_1	R_2	r	C_1	C_2	ρ	β
1)	Non Tapered	3.7	3.7	1	500	500	1	2.8
2)	Impedance Tapered	3.7	14.8	4	500	125	4	2.05
3)	Part. Tapered (r=1)	7.4	7.4	1	500	125	4	1.4
4)	Part. Tapered (ρ=1)	1.85	7.4	4	500	500	1	5.6
5)	r=1 and min. GSP	10	10	1	435.2	78.07	5.53	1.28
6)	R-Tapered, min. GSP	10	40	4	340.4	25.16	13.52	1.26
7)	C-Tapered, min. GSP	5.45	10.06	1.85	500	125	4	1.58
8)	Strongly C-Tap, min. GSP	5.78	23.64	4.09	500	50	10	1.38

Observing the E_{nef} column, i.e. the RMS noise voltage over the frequency range $\Delta\omega$, we conclude that the filter with the lowest noise is filter Nr. 8), i.e. with strong capacitive tapering and minimum Gain-Sensitivity Product (GSP). The second best results are obtained with filter Nr. 3), i.e. a partially tapered filter with equal resistors (r=1).

The same filter circuits as in Table II are referred to in Table III. As stated earlier, in the last two columns, the results of a Monte Carlo sensitivity analysis as discussed in [5] is given. Observing the $\sigma_{\alpha}(\omega_p)$ column, i.e. the standard deviation of the filter's magnitude at the pole frequency ω_p , one can conclude that the filter with the lowest sensitivity to component tolerances is filter Nr. 6) with resistive tapering and minimum GSP (marked with bold border). The next best results are C-tapered filters with minimum GSP, and partially tapered filters with equal resistors (r=1).

TABLE III
NOISE CHARACTERISTICS, MAGNITUDE MEAN VALUE AND STANDARD DEVIATION OF FILTERS GIVEN IN TABLE II (V_{nmax} IN [nV/√Hz], E_{nef} IN [μV], D_R , $\bar{\alpha}(\omega_p)$ AND $\sigma_{\alpha}(\omega_p)$ IN [DB])

Nr.	Filter	V_{nmax}	E_{nef}	D_R	$\bar{\alpha}(\omega_p)$	$\sigma_{\alpha}(\omega_p)$
1)	Non Tapered	849.07	185.94	85.58	23.26	3.36
2)	Impedance Tapered	502.46	114.58	89.79	20.23	1.99
3)	Partially Tapered (r=1)	425.77	93.38	91.56	16.85	1.38
4)	Partially Tapered (ρ=1)	1756.9	385.33	79.25	29.64	4.80
5)	r=1 and min. GSP	447.19	95.51	91.37	16.39	1.19
6)	R-Tapered and min. GSP	442.33	98.75	91.08	15.79	0.93
7)	C-Tapered and min. GSP	428.84	94.44	91.47	18.12	1.57
8)	Strongly C-Tap, min. GSP	389.54	88.06	92.07	16.62	1.13

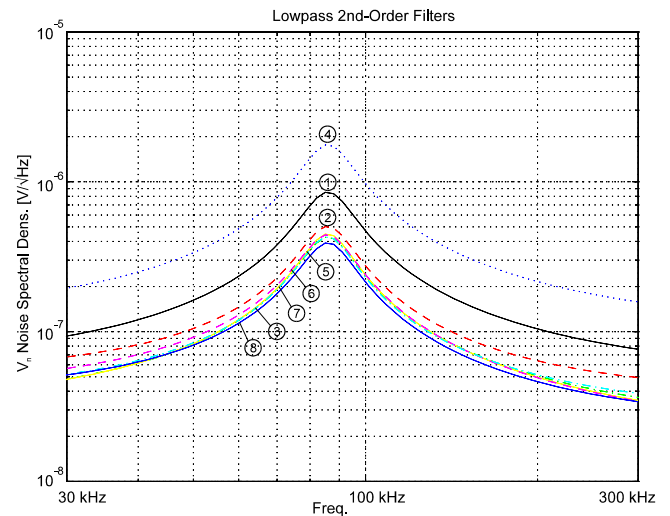


Fig. 4. Noise Spectral Density of Second-order Low-Pass Filters given in Table II

We see that the sensitivity analysis results coincide with the noise analysis results. A first conclusion is that impedance tapering minimizes both the sensitivity to component tolerances and the noise contribution at the filter output. Note that the partially tapered filter with equal resistors ($r=1$) (Nr. 3) has a significantly lower sensitivity to component variations, and an improvement in noise characteristics, compared with the non-tapered standard circuit (Nr. 1). The R-tapered and min. GSP filter (Nr. 6) shows an even lower sensitivity. Considering only the noise analysis, good results are obtained with $r=1$ and min. GSP (filter Nr. 5) and C-tapered and min. GSP (filter Nr. 8). The output voltage noise spectral density for each filter of Table II is shown in Fig. 4.

Thus, in summary, for the general second-order low-pass filter, partial impedance tapering with equal resistors ($r=1$), or equal resistors and capacitor values selected for GSP-minimisation, provide circuits with a minimum sensitivity to the component tolerances of the circuit and a significant noise reduction. For higher demands on noise, it is recommended to strongly capacitively taper the circuit and select resistor values for GSP-minimisation.

B. Second-order High-Pass Filters

Consider the second-order high-pass filter shown in Fig. 5.

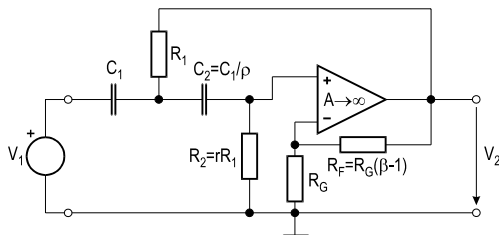
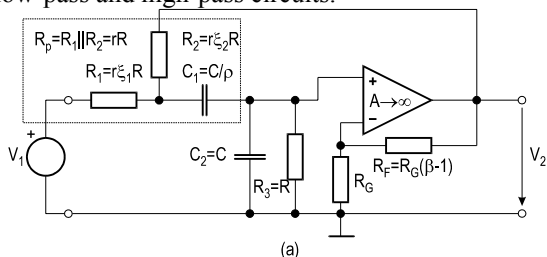


Fig. 5. Second-order High-pass Filter.

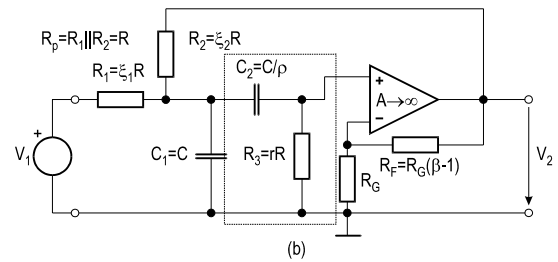
For the high-pass circuit the same noise and sensitivity analysis as for the low-pass circuit was performed. Since the circuits are dual, the obtained results show that *capacitive impedance tapering with resistors values selected for GSP-minimisation, provide circuits with a minimum sensitivity to the component tolerances of the circuit and a significant noise reduction.*

C. Second-order Band-Pass Filters

Two realizations of second-order band-pass filters are presented in Fig. 6. The realization Type B is superior, thus Type A will not be considered. The obtained results show that the band-pass circuit produces higher output noise than the low-pass and high-pass circuits.



(a)



(b)

Fig. 6. Second-order Band-pass Filters. (a) Type A. (b) Type B.

Thus, in summary, similar to the high-pass circuit, *capacitive impedance tapering with resistors values selected for GSP-minimisation, provide circuits with a minimum sensitivity to the component tolerances of the circuit and a significant noise reduction.*

IV. CONCLUSION

It is shown that active resistance-capacitance (RC) low-pass filters designed for low-sensitivity to component tolerances are also low in output thermal noise. A procedure for the design of low-sensitivity allpole filters of second and third order has been previously published [5, 7]. The filters are of low power because they use only one OA. The design procedure using impedance tapering adds nothing to the cost of conventional circuits; the component count and topology remains the same, only component values change. The extension to third- and higher-order filter sections follows precisely the same principles, and will be reported on shortly. Using low-noise OAs and metal-film resistors together with the proposed design method, low-sensitivity, low-noise filters result.

REFERENCES

- [1] J. Zurada and M. Bialko, "Noise and Dynamic Range of Active Filters with Operational Amplifiers," IEEE Trans. on Circuits and Systems, vol. CAS-22, no. 10, pp. 805-809, Oct. 1975.
- [2] N. Stojković and N. Mijat, "Noise and dynamic range of second order OTA-C BP filter sections," Proceedings of the European Conference on Circuit Theory and Design ECCTD '99 (Stresa, Italy), 1999, 795-798.
- [3] P. Bowron and K. A. Metzher, "The Dynamic Range of Second-Order Continuous-Time Active Filters," IEEE Trans. on Circuits and Systems, vol. 43, no. 5, pp. 370-373, May 1996.
- [4] R. Schaumann, M. S. Ghauri and K. R. Laker, Design of Analog Filters-Passive, Active RC and Switched Capacitor. New Jersey 07632, Prentice Hall, Englewood Cliffs, 1990.
- [5] G. S. Moschytz, "Low-Sensitivity, Low-Power, Active-RC Allpole Filters Using Impedance Tapering," IEEE Trans. on Circuits and Systems, vol. CAS-46, no. 8, pp. 1009-1026, Aug. 1999.
- [6] D. Jurišić and G. S. Moschytz, "High-Pass and Band-Pass Low-Sensitivity, Low-Power, Active-RC Allpole Filters Using Impedance Tapering," Submitted for publication to IEEE Trans. on Circuits and Systems.
- [7] G. S. Moschytz, "Realizability constraints for third-order impedance-tapered allpole filters," IEEE Trans. on Circuits and Systems, vol. CAS-46, no. 8, pp. 1073-1077, Aug. 1999.
- [8] R. P. Sallen and E. L. Key, "A practical Method of Designing RC Active Filters," IRE Transactions on Circuit Theory, vol. CT-2, pp. 78-85, 1955.
- [9] G. S. Moschytz, Linear Integrated Networks: Design. New York (Bell Laboratories Series): Van Nostrand Reinhold Co., 1975.